Bio-Radar Cardiac Signal Model Used for HRV Assessment and Evaluation Using Adaptive Filtering

Carolina Gouveia, *Graduate Student Member, IEEE*, Daniel Filipe Albuquerque, Pedro Pinho, *Senior Member, IEEE*, and José Vieira

***Abstract*— The ability to remotely assess vital signs using radar systems may potentialize the healthcare systems, since it does not require any direct interaction with the subject. Nonetheless, these systems present inherent challenges that could compromise the accuracy of the vital signs parameters. For instance, there is a lack of resolution on the cardiac signal, since the radar only detects the chest micro-displacement. Low cardiac resolution prevents the exact localization of signal peaks, compromising the heart rate variability (HRV) assessment. In this work, we use a customized bandpass filter (BPF) obtained through adaptive filtering, applied to the electrocardiography (ECG) signal to generate the corresponding synthetic radar signal. This provides an easy way to extract a cardiac radar signal model, free of issues that arise from random body motion (RBM) or from an eventual decrease in signals quality, which are inherent issues of long-term acquisitions. This model was further used to verify if the signal resolution provided by lower carrier radars is suitable to determine the HRV parameters accurately.**

***Index Terms*— Bio-radar, cardiac signal, continuous wave (CW), Doppler radar, heart rate variability (HRV), vital signs, Wiener filter.**

I. Introduction

THE bio-radar system is a non-contact technology able to monitor remotely the respiratory and the cardiac signal [1]. The bio-radars implemented with continuous-wave (CW) radar are based on the micro-Doppler effect. A radio frequency (RF) signal is transmitted toward the subject's chest wall, which moves periodically due to the cardiopulmonary function. The RF signal is reflected on the chest wall and subsequently received by the radar front-end, being phase modulated due to that periodical motion [2].

The received signal contains both respiratory and cardiac signals, wherein the cardiac component extraction from a radar signal is a challenging task. This fact is related not only to radar operation limitations, but also due to the proper nature of the cardiopulmonary function captured by the radar. First of all, the received signal presents a spectral proximity of both respiratory and cardiac components, and an eventual harmonic superposition. Several methods have been proposed in the literature to separate both bio-signals, which encompass spectral manipulation [3], filtering [4], and signal decomposition [5], [6]. A multiresolution analysis using wavelets is also an effective method as proved in [7]–[13].

With regard to the way bio-signals are perceived by the radar, the respiratory stands out as the dominating signal, with an amplitude varying between 4 and 12 mm [14], while the maximum displacement due to heartbeat consists of 0.5 mm [15]. Ramachandran and Singh [15] used laser speckle interferometry to measure the corresponding chest-wall motion to each electrocardiography (ECG) wave, and they observed that the highest motion is related to the Q-wave, R-wave, S-wave (QRS) complex of the ECG and is focused in one specific location, namely, the apex of the heart. Hu *et al.* [7] also pointed out that identifying that area is increasingly hampered if the subject is not at rest or if the radar antenna is not properly focused on that maximal displacement zone. This fact can be worsened if directional antennas are being used, since narrow beam widths require a precise alignment. It should be noted that directive antennas are, in fact, the most indicated, especially in CW radars to avoid the reception of parasitic reflections that occur in the surrounding environment [16]. In addition, the chest-wall motion amplitude and the cardiac signals quality are also related to subjects physiognomy and gender [7], [17], [18].

The bio-radar potential can be maximized if the acquired bio-signals are used to infer certain subject conditions such as, the emotional state, drowsiness or to help identify possible cardiopulmonary diseases. For this purpose, beside the signals rate, other parameters can be estimated as the heart rate variability (HRV). The HRV enables to assess the cardiac vagal tone, which marks the contribution of the parasympathetic nervous system to the cardiac regulation [19], allowing our body adaptation to sudden psychophysiological modifications required to guarantee the homeostasis [20]. While the heart

Manuscript received 4 March 2022; revised 6 June 2022; accepted 21 June 2022. Date of publication 12 July 2022; date of current version 19 July 2022. This work was supported in part by the Fundação para a Ciência e Tecnologia (FCT) through the Fundo Social Europeu (FSE) and the Programa Operacional Regional do Centro under Ph.D. Grant SFRH/BD/139847/2018, in part by FCT/Ministério da Ciência, Tecnologia e Ensino Superior (MCTES) through the national funds and when applicable co-funded the European Union (EU) Fund under Project UIDB/50008/2020-UIDP/50008/2020 and Project UIDB/05583/2020, in part by the Research Centre in Digital Services (CISeD), and in part by the Polytechnic of Viseu. The Associate Editor coordinating the review process was Dr. Dong Wang. *(Corresponding author: Carolina Gouveia.)*

This work involved human subjects or animals in its research. Approval of all ethical and experimental procedures and protocols was granted by the Ethics and Deontology Committee of University of Aveiro, Aveiro, Portugal, under Approval No. 29-CED/2021.

Carolina Gouveia, Pedro Pinho, and José Vieira are with the Departamento de Eletrónica, Telecomunicações e Informática, Universidade de Aveiro, 3810-193 Aveiro, Portugal, and also with the Instituto de Telecomunicações, 3810-193 Aveiro, Portugal (e-mail: carolina.gouveia@ua.pt; ptpinho@ua.pt; jnvieira@ua.pt).

Daniel Filipe Albuquerque is with the Centro de Investigação em Serviços Digitais (CISeD), Escola Superior de Tecnologia e Gestão de Viseu (ESTGV), Politécnico de Viseu, 3504-510 Viseu, Portugal (e-mail: dfa@estgv.ipv.pt).

Digital Object Identifier 10.1109/TIM.2022.3190035

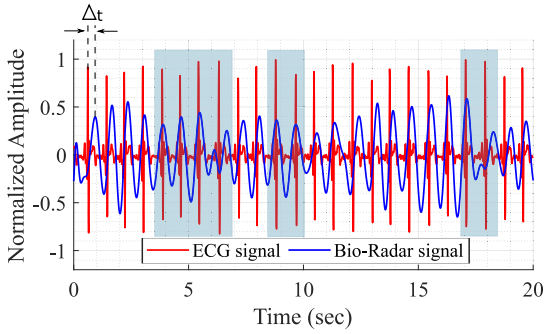

Fig. 1. Illustration of the radar peaks time location variation [13].

rate indicates the number of beats per minute (BPM), the HRV measures the variation of the interbeat interval (IBI) [19], [20]. To obtain such delicate parameters, a cardiac signal with high resolution is required to correctly identify cardiac peaks location.

However, it is challenging to obtain accurate IBI results when the cardiac detection is performed at the chest surface, as suggested by Kaisti *et al.* [17], where they studied the measurement process of the heart mechanical motion. The radar signal acquisition is based on the same principle, but it has an aggravating factor, which is the system sensitivity dependency with the selected carrier frequency. Li *et al.* [16] established a relation between the signal resolution and the carrier frequency selection. They evaluated the relation between the cardiac signal-to-noise ratio (SNR) and the carrier frequency, concluding that frequencies between 5 GHz and the lower region of *Ka*-band provide signals with better SNR.

In this sense, the works presented in the literature so far have been showing interesting results regarding the HRV assessment using radar systems operating with different carriers. Kim *et al.* [21] and Massagram *et al.* [22] using the 2.45-GHz ISM band revealed that HRV parameters cannot be inferred accurately due to intrinsic characteristics of the radar sensor [21], [22]. In [23], this lack of signal resolution is also reported for a radar operating with the same frequency, but an autocorrelation-based algorithm is developed to rectify the missed peaks. Gouveia *et al.* [13] presented a study focused on the cardiac signal extraction on CW radars operating at 5.8 GHz. Six different methods were applied in radar signals, and their effectiveness to extract the cardiac signal was compared. In addition, a preliminary study was carried out to evaluate the feasibility to compute HRV parameters. For this purpose, the time localization of the radar cardiac peaks was inspected. Fig. 1 presents a radar cardiac signal superimposed with an ECG signal captured simultaneously. In general, the radar cardiac peak is delayed in relation to the ECG peak, with a Δ_t time difference. Nonetheless, one can observe that Δ_t varies over time, achieving, in some cases, a value close to zero, when the radar peak superimposes the ECG one (as depicted by the blue regions in Fig. 1). This effect might be related to the lack of signal resolution and leads to an increased variation on the IBI computation.

On the other hand, accurate HRV results were reported mostly using 24-GHz radars in [24]–[27], and as far as we know, [7] is the only work reporting HRV results using a 5.8-GHz radar. Despite the outstanding results presented for 24-GHz radars, one should highlight the importance of performing studies with lower carriers. Higher carriers might require a more complex hardware, their increased sensitivity turn signals prone to be highly affected by random body motion (RBM) during the monitoring period, and high carrier signals also suffer from high attenuation. On the other hand, if lower carriers are used, the overall system becomes simpler, and the interference caused by RBM is less prominent. Furthermore, low carriers allow the operation at a wider range, since their signals are less attenuated. Finally, the research on this scope should also care with the challenges of implementing solutions to be further used in the market. For instance, low-profile systems can be accomplished by hiding the radar inside specific objects. Low-frequency carriers allow this integration, since electromagnetic waves can easily penetrate dielectric materials.

In summary, the accuracy of the cardiac radar signal can be compromised due to different causes, such as the following: 1) the own system sensitivity; 2) the alignment between the subject's chest wall and the maximum lobe of the antenna; 3) the subject stability during the measurement period; and 4) or even the noise interference acquired within the same frequency band. Accordingly, this work aims to simulate the signals acquisition in an ideal scenario, which are not influenced by those external disruptive sources, and verify if under these ideal circumstances, it is possible to compute the HRV parameters using a CW radar operating at 5.8 GHz. For this purpose, an exclusive tool was used, which is fully dedicated to the authentic and unbiased cardiac signal. This tool consists of a radar cardiac signal model, extracted directly from an ECG, using a customized bandpass filter (BPF). In this way, the radar signal model does not encompass any RBM or any other issues presented earlier.

The necessary BPF coefficients were defined using an adaptive filter, namely, the Wiener filter [28]. For this purpose, an ECG signal was used as an input, and a cardiac radar signal acquired at the exact same time was used as its output. Since the estimation robustness must be guaranteed, a study was performed regarding the correlation between the estimated radar signal (ERS) and the corresponding original radar signal (ORS). The correlation variability over time was verified, for different heart rates from the same subject and in-between different subjects.

In summary, our contributions are as follows.

1) Evaluate if it is possible to assess HRV parameters accurately using our bio-radar system setup, operating in CW at 5.8 GHz and implemented through an off-the-shelf RF front-end.
2) The HRV assessment is performed using an ideal cardiac radar signal obtained through adaptive filtering, applied directly to the ECG signal. Under these conditions, external and random sources of noise, such as the body motion or an eventual SNR decrease, cannot compromise the HRV results.
3) The HRV assessment evaluation is performed considering real case scenarios: the signals were acquired

during long time periods (approximately one hour), on different days, in two different subjects and under different psychological conditions.

This work is divided as the following: in Section II, the radar system setup is described, as well as the conducted signal acquisition sessions. In this section, the digital signal processing (DSP) algorithms applied to extract the ORS are also detailed. Then, Section III presents the adaptive filter implementation and its general validation through the study of the correlation variability considering different subjects and different days. Results regarding the heart rate and HRV obtained by ERS are discussed in Section IV, and the final conclusions are presented in Section V.

II. Radar System Setup Description

A. Signals Acquisition

The radar setup used to collect the subjects vital signs was composed by a software-defined radio as RF front-end, namely, the USRP B210 board from Ettus Research[1], operating in CW mode with a 5.8-GHz carrier frequency. Transmission and reception were performed using two 2×2 antenna arrays [13]. These antennas are circularly and crossed polarized, to avoid the mutual coupling and to improve the path gain, according to [29] and [30]. Both antennas have a half-power beamwidth of 40°, and 11.6 dBi of gain. The setup was operated with a transmitted power equal to 2 dBm.

The USRP B210 board was selected as RF front-end for being compact and flexible, meeting the market requirements. Nonetheless, the USRP presents some hardware limitations when it is being used in radar applications, such as phase incoherency between the transmitting and receiving channels and also a weak isolation between both ports. One should note that these hardware issues will not affect the results herein reported, since the DSP algorithm used to extract the vital signs was developed to overcome these issues. The algorithms are explained further in detail in Section II-B.

An informed consent was obtained from all the subjects. To account with the individual differences, two subjects were considered in this study: subject 1 and subject 2. The signal acquisition was performed with the subjects seated in front of the antennas at a distance of half meter, while they were watching videos. The videos content was specially selected to induce different emotions, namely, a neutral condition and the fear state [31]. The experiment was conducted in two sessions occurring on separate days, one per emotion, to obtain unbiased and authentic reactions. The same setup configuration and the surrounding environment conditions were kept for all the acquisitions.

Each session was composed by a baseline (which also served as neutral condition) and an inducing moment, to gather time and rate variation for the same subject. These emotions, in turn, induce different HRV parameters [19], which will be determined later for ERS, ORS, and ECG, to evaluate if it is feasible to use this radar setup for this purpose. Considering the emotions induction and the individual behavior in different days, three different moments are going to be evaluated: BL1—Baseline (neutral condition) acquired on the first day, F1—fear condition induced on the first day, and N2—neutral condition induced on the second day.

[1]Trademarked.

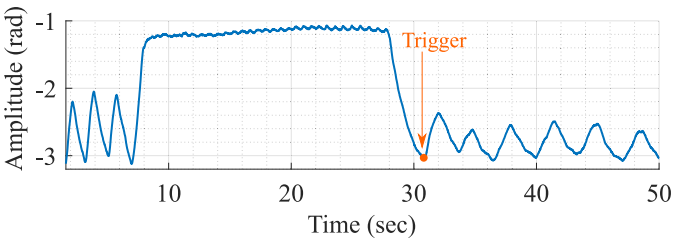

Fig. 2. Breathing pattern and trigger definition for signals synchronization.

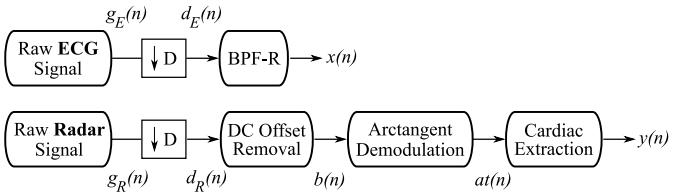

Fig. 3. Signal processing algorithm for the wiener coefficients estimation.

The vital signs were acquired simultaneously, using our bio-radar prototype and the BITalino (r)evolution BT board for the ECG signal [32]. To synchronize both signals, the subjects were asked to perform a breathing pattern composed by three deep breaths, an apnea period of 10 s and a slow exhale, as depicted in Fig. 2. Then, immediately before the next inhale, the subject pushed a trigger button to start the ECG acquisition. On the post-processing side, signals are synchronized by neglecting the signal prior to the trigger sample indicated in Fig. 2. In the exact context of this work, where adaptive filtering is being used, it is imperative to assure the system causality. Therefore, the radar signal was considered to start 100 ms before its trigger, to guarantee that in case of synchronization doubt, it is delayed in relation to the ECG signal.

After their acquisition, both ECG and radar signals were processed before being used as input and output, respectively, on the Wiener filter. Section II-B details the DSP algorithm implementation.

B. Radar Signal Processing Algorithm

Fig. 3 shows the block diagram of the implemented DSP algorithm. The bio-radar signal $g_R(n)$ was acquired using the GNU Radio Companion software, with a sampling frequency equal to 100 kHz, and the ECG signal $g_E(n)$ was acquired using the OpenSignals software, from PLUX, with a sampling frequency equal to 1 kHz. Both signals were processed using MATLAB. First, both were downsampled to operate at a sampling rate of 100 Hz, resulting in $d_E(n)$ and $d_R(n)$ signals. To make the R-peak more prominent, a 15th-order bandpass FIR filter (BPF-R) was applied to $d_E(n)$, between 6 and 20 Hz, as recommended in [33]. In this stage, the resulting ECG signal is the one used as the Wiener filter input $x(n)$.

On the radar side, since a CW radar was used as RF front-end, signals are downconverted to baseband using in-phase

and quadrature demodulation. Thus, the signal processing is performed using complex signals, and the received baseband signal can be represented by an arc projected in the complex plane [1]. Regarding the signal processing steps, first of all, the environment clutter must be removed, since it induces dc offsets in the complex signal. Note that the eventual crosstalk occurring between the transmitting and receiving ports could also increase these dc offsets. The clutter removal can be accomplished by following the algorithm proposed in [1], which is robust to low amplitude signals and to non-static parasitic reflections. In this way, dc offsets are estimated over time encompassing the scenario changes properly. Afterward, the hardware phase incoherence is compensated by rotating the arc signal $b(n)$ to vary around 0° phase. Finally, the vital signs information is extracted through a phase demodulation by applying the arctangent demodulation [34]. Thus, the signal $at(n)$ contains both respiratory and cardiac signals, which are then separated in the cardiac extraction block. Herein, it is used a BPF combined with discrete wavelet transform (DWT) [13]. We verified, in preliminary tests, that applying a BPF prior to DWT attenuates the respiratory component and improves the resultant cardiac signal [13]. In this case, the BPF is a 100th-order FIR filter, with a passband between 0.7 and 2 Hz. The filter order was selected considering a 10-dB attenuation over the respiratory frequency band. On the other hand, the DWT coefficients are obtained using the maximal overlap discrete wavelet transform, implemented with *modwt* function from MATLAB, considering seven decomposition levels [10]. The selected mother wavelet was the Daubechies with four vanishing moments. The resultant signal $y(n)$ was recovered from the wavelet coefficients using the *modwtmra* function from MATLAB, using only the 5th and 6th decomposition levels [13].

III. Adaptive Filter Implementation Using the Wiener Filter

A. Wiener Coefficients Estimation Using a Short-Time Signal

The ECG signal can be seen as a sum of waves, correspondent to the different heartbeat phases: the P-wave, QRS complex, T-wave, and U-wave [35]. On the other hand, the cardiac radar signal is obtained from the measurement of the mechanical motion of the heart, and thus, its rate can be comparable with the fundamental component of the ECG signal.

This fact can be verified in Fig. 4, which shows an example of a radar and an ECG signals spectrum, normalized according to their maximum magnitudes to ease the analysis. These signals were acquired at the exact same time and for the same subject. Fig. 4 presents the radar signal spectrum in two different stages of the algorithm previously presented in Fig. 3. The black dashed black line shows the spectrum of the $at(n)$ signal, after removing the dc offsets of the radar signal, and yet containing the respiratory component. The blue line shows the spectrum of the cardiac radar signal $y(n)$.

Starting with the radar spectrum ($at(n)$ signal), in Fig. 4, it is possible to identify the respiratory and cardiac spectral components. Both components are aligned in frequency with the ECG spectrum. For instance, the respiratory peaks stand in

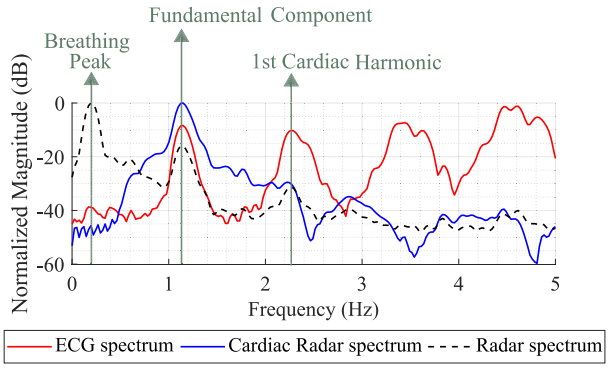

Fig. 4. Normalized ECG and radar signals spectrum for different stages of the radar DSP.

the 0.244 Hz (equivalent to 14.6 breaths per minute), and the fundamental cardiac component stands in 1.123 Hz (equivalent to 67.4 BPM) for both radar and ECG signals. The radar signal presents a higher magnitude in the respiratory spectral component, since this signal has an amplitude ten times higher than the cardiac one. More specifically, the radar cardiac component is attenuated almost 20 dB in comparison with the respiratory one. Conversely, the ECG spectrum consists of a set of well-defined harmonics, with high magnitude, inherent to the aforementioned signal nature. The overall radar spectrum matches with the ECG one in the fundamental component and in the first harmonic. The same behavior is observed for the $y(n)$ radar signal, where the respiratory component is fully mitigated.

In this work, we aim to extract a radar cardiac signal model from the ECG, to further inspect if it possible to compute HRV parameters without the influence of RBM and eventual SNR decrease. For this purpose, the first stage of this work is to find the filter coefficients $W(n)$ that can relate an ECG signal with the cardiac radar signal acquired at the exact same time, and this can be performed using adaptive filtering. The Wiener filter was selected for being a FIR filter, as it presents a stable behavior. Based on a least-squared error approach, the wiener coefficients are computed to minimize the average-squared distance between the filter output and input [28] and, thus, determine the transfer function $H(n)$ that relates both signals. In practice, the transfer function $H(n)$ represents the channel model between the ECG signal and the ORS. The implementation of the Wiener filter to determine $W(n)$ is depicted in Fig. 5(a).

According to [28], the Wiener theory assumes that signals are stationary. Therefore, the values of $W(n)$ are determined using short time signals, namely, with 1-min duration to always guarantee a good approximation. The radar signal for a single subject can vary largely over time, especially in the long-term acquisitions due to RBM that the subject might perform for discomfort reasons. Therefore, the 1-min segment was carefully selected keeping in mind that it should provide the best correlation result between the ORS and the ERS over time. The selection of such 1-min segment and the further filter implementation were carried out through two different approaches for each subject: A1—a single 1-min segment was selected to compute the $W(n)$ once, and the same filter was

TABLE I
MEAN CORRELATION RESULTS FOR DIFFERENT FILTER ORDERS

Radar Signal	Subject 1						Subject 2					
	BL1		F1		N2		BL1		F1		N2	
	A1	A2	A1	A2	A1	A2	A1	A2	A1	A2	A1	A2
O = 512	0.85	0.87	0.72	0.74	0.79	0.81	0.74	0.74	0.70	0.71	0.59	0.70
O = 1024	0.84	0.86	0.71	0.73	0.77	0.80	0.72	0.74	0.68	0.71	0.59	0.71
O = 2048	0.83	0.85	0.70	0.72	0.58	0.79	0.69	0.72	0.66	0.72	0.58	0.71
O = 4096	0.80	0.82	0.67	0.74	0.61	0.77	0.68	0.72	0.59	0.71	0.54	0.78

BL1 - baseline day 1, F1 - fear day 1, N2 - Neutral condition day 2, O - filter order, A1 - fully static system, A2 - five-minutes updated static system

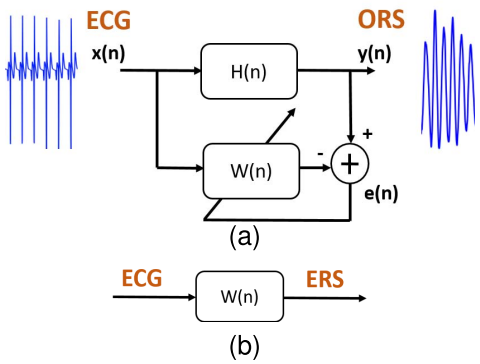

Fig. 5. Illustration of the procedure to obtain the ERS. (a) Wiener filter implementation to determine $W(n)$ coefficients, to be further used in the transfer function $H(n)$. (b) Application of the bandpass filter to obtain the ERS.

applied over time. For this case, the BL1 was analyzed seeking for a moment free of RBM; A2—all signals were divided into 5-min segments and the 1-min segment that provided the best correlation for its 5-min slot was selected. In this way, the values of $W(n)$ are updated every 5 min, leading to a different filter for each instance. This periodicity was selected, since signals with a minimum duration of 5 min are required for the HRV parameters computation [20].

It was also selected a total number of 1024 coefficients, for being an exponent of power 2 and having in mind an optimal resolution in frequency, but yet a reasonable order to further compensate the caused delay. Moreover, the same number of points was used in the Welch method to obtain the signals spectrum. It is important to note that the selected number of coefficients was the result of a series of trials that encompass low and higher order approaches. Almost all trials presented similar correlation results, as demonstrated in Table I, and therefore, 1024 was selected considering a balance between the delay compensation and the spectral resolution.

As an example, Fig. 6 shows the frequency response of the resulting $W(n)$ using the A1 approach. To approximate the ECG signal to the radar one, $W(n)$ presents a magnitude equal to 30 dB around the fundamental cardiac component, since the ECG fundamental component is attenuated that the same amount in relation to the radar. On the other hand, $W(n)$ attenuates the first harmonic around 20 dB, and the remaining ECG spectral harmonics are attenuated more than 30 dB. After determining $W(n)$, the ERS can be obtained and compared

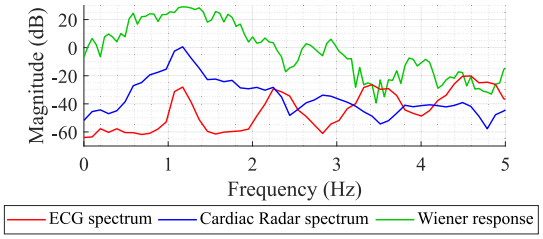

Fig. 6. Wiener coefficients behavior in frequency domain along with the corresponding ECG and ORS spectrum.

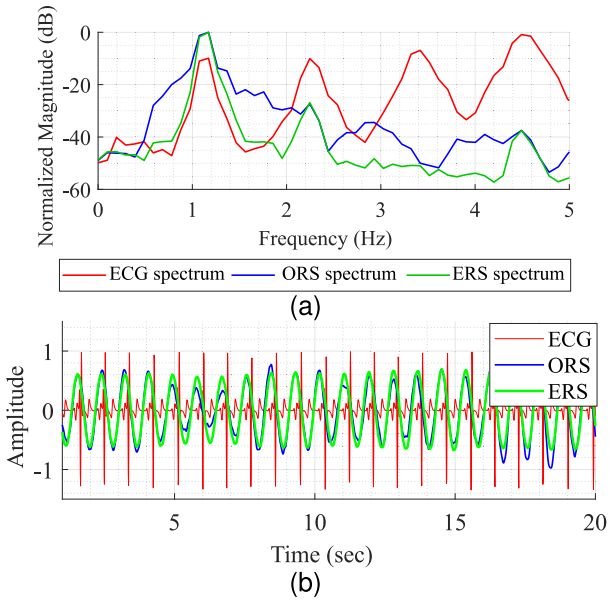

Fig. 7. Evaluation of the obtained estimated radar signal. (a) Normalized spectrum of ERS, ORS, and ECG signals. (b) Time domain signals.

with the ORS, by applying a BPF on the ECG signal using $W(n)$ [see Fig. 5(b)]. Then, the filter delay was compensated, and for the subsequently comparison purposes, both ECG and ORS were also compensated assuming the same delay.

Fig. 7 shows the result, where Fig. 7(a) shows the obtained normalized spectrum of ERS, ORS, and ECG, and Fig. 7(b) presents the corresponding superimposed time domain signals. It is possible to verify that the ERS is highly correlated with the ORS in that signal portion. The correlation can be indeed verified, by computing the cross correlation between ORS and ERS, which is equal to 0.95 in this case.

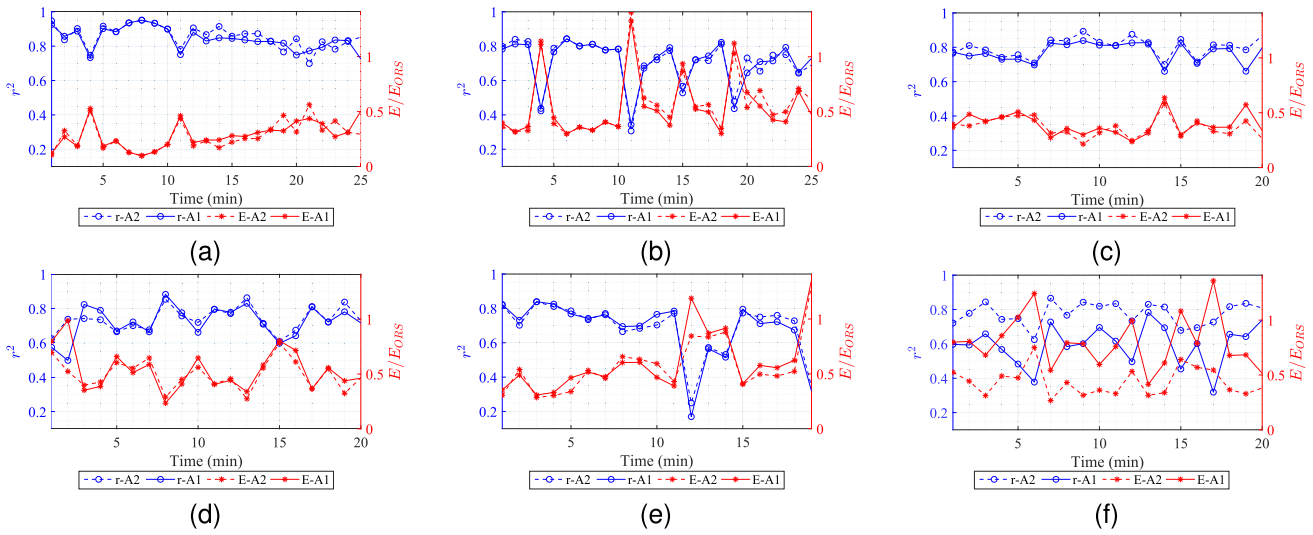

Fig. 8. Cross correlation between ERS and ORS over time and the corresponding residual error on the $W(n)$ estimation for subject 1 and subject 2. (a) and (d) For BL1. (b) and (e) For F1. (c) and (f) For N2.

B. ERS Analysis

Before computing the cardiac signal parameters associated with ERS, it is required to evaluate the correlation between the ERS and ORS over time, for the different subjects in all moments. High correlation demonstrates the similarity of both signals, allowing a reliable analysis. Nonetheless, it is worth to highlight that the purpose of this work is to evaluate the effectiveness of obtaining HRV parameters considering a static system. For these reason, the results of both approaches used for $W(n)$ were analyzed simultaneously, where A1 represents a full static system and A2 represents a system that it is only static during 5 min.

Fig. 8 shows the cross correlation between the ERS and the ORS and the corresponding residual error on the $W(n)$ estimation for different moments: Fig. 8(a) corresponds to BL1; Fig. 8(b) corresponds to F1, and Fig. 8(c) corresponds to N2. The residual error was estimated through the ratio between the energy of the error (ORS–ERS) and the energy of the ORS. Furthermore, Fig. 9 shows the spectral coherence between ERS and ORS, computed at the ORS fundamental frequency.

Starting with the time correlation for subject 1 for the A1 approach, on the BL1 case, the cross correlation is kept above 0.8 most of the time, presenting a mean value of 0.84. Worst correlation results were obtained for the F1 case, where the cardiac rate is changing due to frights, and the occurrence of more RBM is also expected. Even though, some of the correlation results were above 0.8, presenting a mean value of 0.71. The neutral condition on a different day (N2 case) presented also correlation close to 0.8, where the mean value decreased slightly to 0.77. With this results, it is possible to state that ERS and ORS are identical, excepting some differences inherent to heartbeat changes or sporadic involuntary motions, that were not accounted by $W(n)$. For the A2 approach, the results were slightly better, where a correlation of 0.86, 0.73, and 0.80 was obtained for the BL1, F1, and N2 cases, respectively. One can also see that the residual error keeps the correlation pace, increasing when lower correlations were observed and vice versa. More differences between A1 and A2 approaches were observed in the spectral coherence analysis in Fig. 9, where A1 stands out with the worst results, especially on the F1 case. The A1 represents a fully static system, so the eventual physiological changes due to the fear feeling might be hided. Thus, A1 might not represent fully the actual cardiac signal that subject 1 presented that day. On the other hand, A2 keeps track of the cardiac changes that occurred during the experiment, leading to a better match with the ORS signal frequency.

Fig. 8(d)–(f) shows the time correlation results and the corresponding residual errors for subject 2. In this case, the correlation results were worse for both A1 and A2 approaches. Starting with the A1 approach, the BL1 case presented several cases above 0.8, but a higher number of cases around 0.7, leading to a mean value of 0.72. The cases related to the fear condition and the neutral condition on a different day embraced higher variations leading to a mean correlation of 0.68 and 0.59, respectively. On the other hand, A2 stands out with a better correlation, presenting 0.74 for the BL1 and 0.71 for F1 and N2 cases.

The low correlation results of subject 2 for the A1 approach suggest that a reliable analysis requires the estimation of new $W(n)$ coefficients over time, using in this way a block-adaptive approach where Wiener theory can be equally applied, as indicated in [28]. This was somehow accomplished with the A2 approach, by updating the $W(n)$ on every 5 min. Thus, despite the lower correlation obtained in some 1-min segments, we believe that the obtained correlation is, in general, enough to evaluate the heartbeat parameters of the ERS, specially having in mind that the ERS does not contain subject motions and keeps that the same signal quality over time.

IV. Feasibility of HRV Assessment

To validate the usage of radar systems for HRV computation, the number of BPM was first computed over time, as well as its error in relation with ECG. All signal rates were obtained

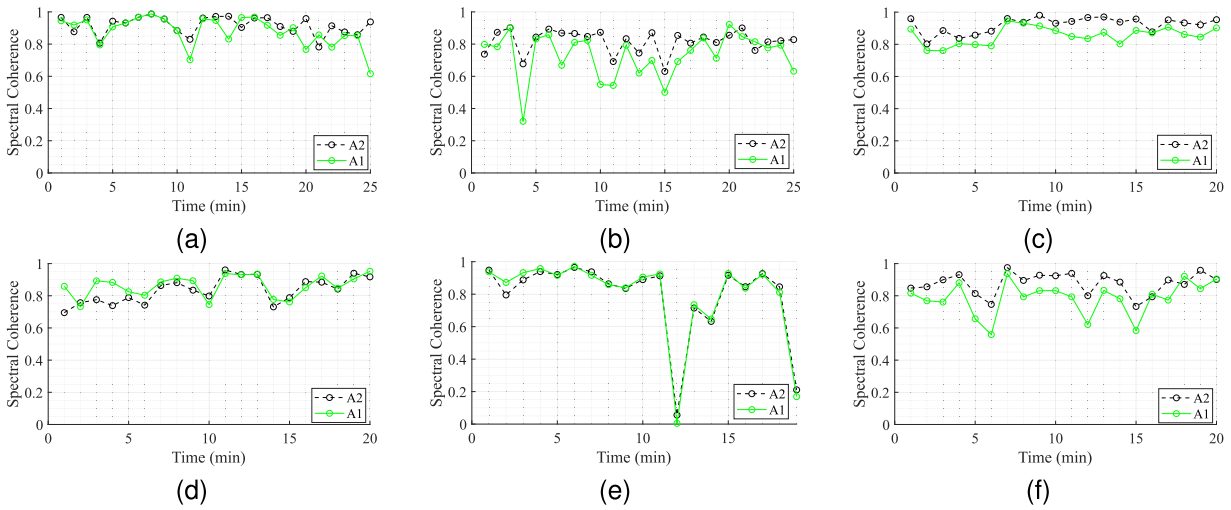

Fig. 9. Spectral coherence between ERS and ORS over time for subject 1 and subject 2. (a) and (d) For BL1. (b) and (e) For F1. (c) and (f) For N2.

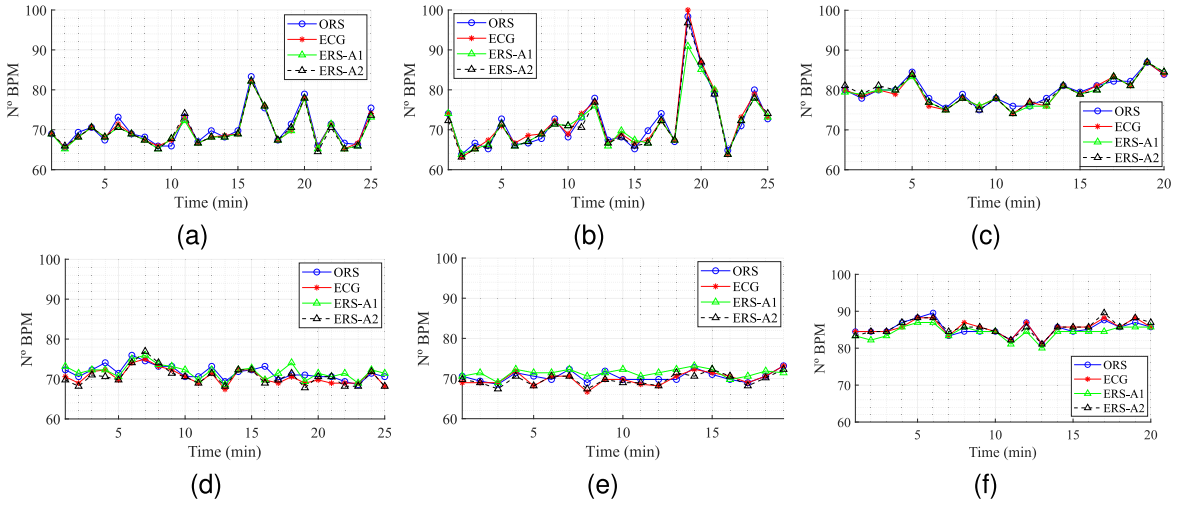

Fig. 10. BPM among ERS, ORS, and ECG over time for subject 1 and subject 2. (a) and (d) For BL1. (b) and (e) For F1. (c) and (f) For N2.

through the IBI estimation. For ORS and ERS signals, the zero-crossing intervals were identified, and a peak was defined by the maximum of such interval. A time threshold was applied to prevent outliers, consisting of half of the mean IBI of the full 1-min segment. Since the ECG signal presents sharped peaks, their identification was easier using only an amplitude threshold. The number of BPM for ECG, ORS, and ERS signals corresponds to the median value of the inverse of IBI values.

Fig. 10 shows the comparison of the BPM among ECG, ORS, and ERS, in the different moments for subject 1 and subject 2. The error behavior of both ORS and ERS was evaluated through its empirical cumulative distribution function, depicted in Fig. 11. Table II presents the error values in BPM taken by 95% of the dataset. More similarity between the three signals can be observed for subject 1. On the other hand, the ERS presented an increased error for subject 2 for the A1 approach. Overall, the ORS presented an error varying between 1.63 and 2.3 BPM. For the subject 1 case, ERS-A1 presented a lower error varying between 0.87 and 2.0 BPM, and the error varied between 0.89 and 2.9 for ERS-A2. A higher error was obtained for subject 2 using the A1 approach, which exceeded 3 BPM. This increased error might be related to the lack of correlation observed previously.

TABLE II
BPM ERROR OF ERS AND ORS FOR EACH SUBJECT ON THE DIFFERENT CONDITIONS

Radar Signal	Subject 1			Subject 2		
	BL1	F1	N2	BL1	F1	N2
ERS-A1	0.87	2.00	1.04	3.08	3.28	2.52
ERS-A2	0.89	2.92	1.07	1.68	1.56	1.24
ORS	1.63	2.19	1.97	2.32	2.30	1.32

BL1 - baseline day 1, F1 - fear day 1, N2 - Neutral condition day 2

The HRV evaluation was focused on the time domain parameters: the standard deviation of IBIs (SDNN) and the root mean square of successive difference of IBI (RMSSD). SDNN

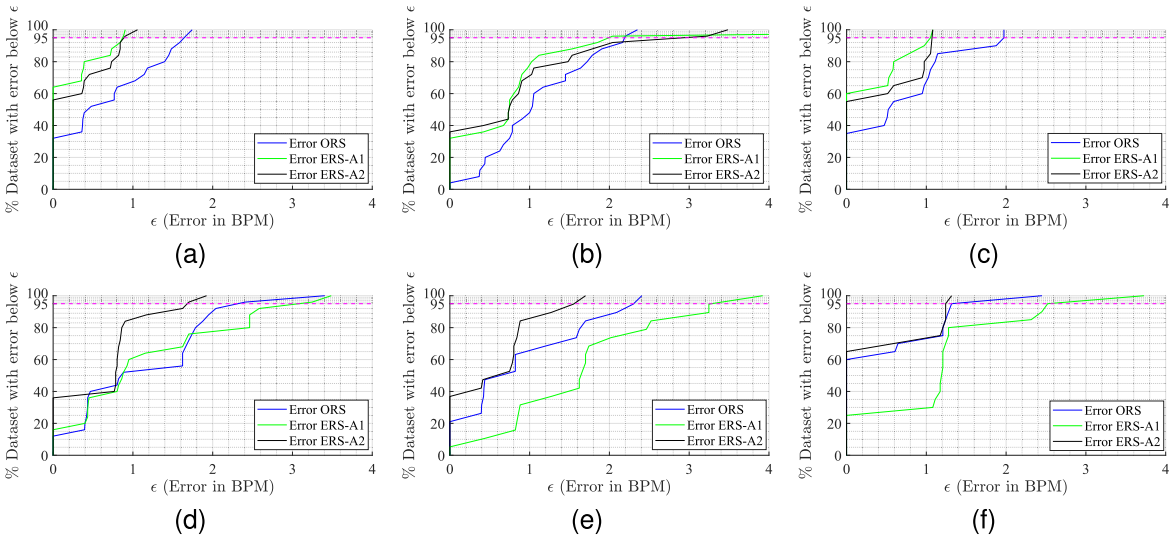

Fig. 11. Empirical cumulative distribution function of the error in BPM for subject 1 and subject 2. (a) and (d) For BL1. (b) and (e) For F1. (c) and (f) for N2.

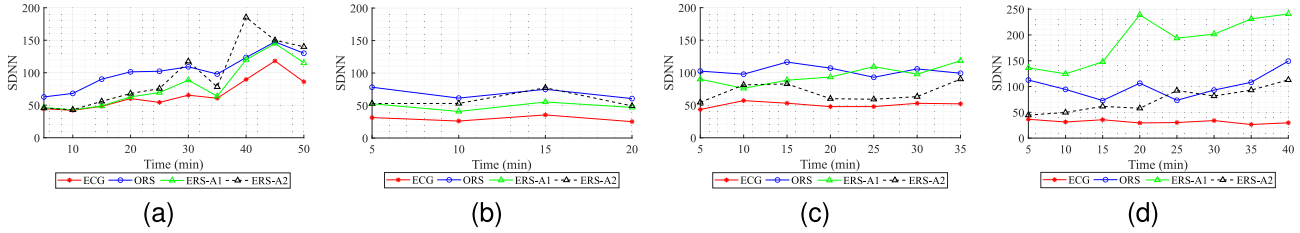

Fig. 12. SDNN (a) using a fear condition of subject 1, (b) using a neutral condition of subject 1, (c) using a fear condition of subject 2, and (d) using a neutral condition of subject 2.

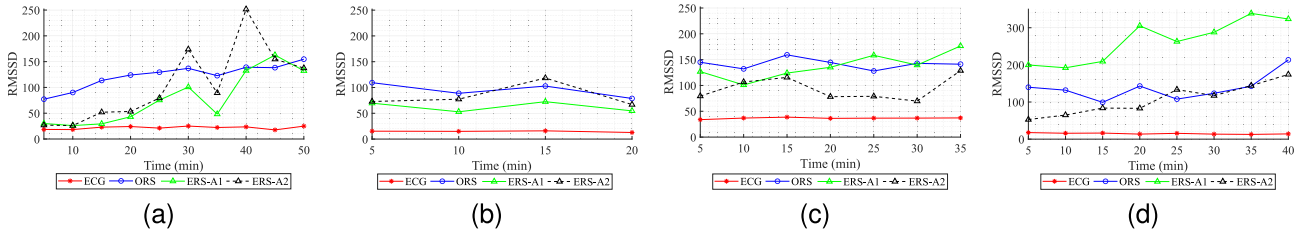

Fig. 13. RMSSD (a) using a fear condition of subject 1, (b) using a neutral condition of subject 1, (c) using a fear condition of subject 2, and (d) using a neutral condition of subject 2.

and RMSSD were computed using the following equations, respectively [19]:

$$\text{SDNN} = \sqrt{\frac{1}{N_{\text{IBI}} - 1} \sum_{i=1}^{N_{\text{IBI}}} \left| \Delta_t[i] - \overline{\Delta_t} \right|^2} \tag{1}$$

$$\text{RMSSD} = \sqrt{\frac{1}{N_{\text{IBI}}} \sum_{i=1}^{N_{\text{IBI}}} (\Delta_t[i] - \Delta_t[i-1])^2} \tag{2}$$

where N_{IBI} is the total of IBIs on the signal segment, $\Delta_t[i]$ corresponds to the IBI value on the ith position, $\Delta_t[i-1]$ is the value on the previous position, and $\overline{\Delta_t}$ is the mean value of all IBIs on the signal segment.

The HRV parameters were computed in the full signals, that included baseline and emotional condition, but divided in 5-min segments according to the guidelines defined in [19]. The obtained results are shown in Figs. 12 and 13. Overall, the HRV parameters computed for the ORS present results largely different from the ones provided by the ECG signal, and the same effect is observed for the ERS signal for both A1 and A2 approaches.

The lack of correlation observed in subject 2 using the A1 approach might influence the HRV results as well, since the error in BPM is often higher than the one obtained with the ORS. Nonetheless, all results obtained for the A2 approach demonstrated generally a higher correlation in both neutral and fear scenarios, and therefore, the HRV results can be more reliable.

Considering exclusively the results obtained for the A2 approach, the results of the same day during the fear condition test for subject 1 [see Figs. 12(a) and 13(a)] start with a high

match with the ones provided by the ECG signal, but cannot keep that similarity over time, reaching values close to ORS or even higher. Likewise, the results obtained for a neutral condition on a different day are equally higher than the ones obtained with the ECG, especially on the RMSSD case.

In subject 2, although the A2 approach presented results closer to the ones obtained for ECG, they were still largely different. These results indicate that the mechanical motion caused by the heart bumping perceived on the chest does not provide enough resolution to obtain accurate results for the HRV parameters. This fact is valid for the front-end and the vital signs extraction algorithm described in Section II. This conclusion was raised with the fact that the ERS is directly extracted from an ECG signal, which means that does not encompass radar problems, such as the subject random motion or the temporary misalignment with the front-end. In this way, it is assumed that the acquisition conditions are kept over time.

Furthermore, it was also observed that radar signal models derived using a Wiener filter through the A2 approach presented a trustworthy behavior when signals are stable over time. Dynamic signals alter the correlation with the ORSs, which can directly affect the cardiac parameters further computed, hence providing biased results.

V. Conclusion

To accurately compute HRV parameters, high resolution signals are required using ECG, to exactly identify the beating peaks and accurately compute the time interval between peaks. Radar bio-signals contain the chest-wall displacement due to the cardiopulmonary function, and the cardiac signal is specifically obtained by the tenuous mechanical motion that can be perceived on the chest surface. This cardiac micro-motion lacks of resolution by itself, but it might be enough for radars operating with higher carriers. In addition, long-term monitoring periods encompass other damaging effects, such as the RBM or the misalignment with the antennas beams, which decreases the signal quality. Under these conditions, it is difficult to verify if lower carriers can provide accurate HRV parameters. In this sense, the radar cardiac model derived from ECG, which do not encompass those external issues, might be a useful tool to verify if is it possible to compute HRV parameters using to the proposed front-end. This signal model was obtained using a Wiener filter, which generate bandpass coefficients to approximate the ECG signal to a given real radar signal, acquired on the exact same time.

To simultaneously guarantee the system stability and the track of the subject behavior, two approaches were explored to extract the Wiener filter coefficients. One approach considered a fully static system, and the other updated the filter coefficients on every 5 min, respecting the signal duration required to compute HRV parameters. The results of both approaches were compared, showing that reliable results are only obtained if the ERS is similar to ORS. This was not verified for the fully static system model. The Wiener filter can provide trustworthy models, if the radar signal at hand is stable over time. Otherwise, low correlation could indicate misleading heart rates and, hence, biased HRV parameters. This fact can be even more pronounced in cases where the subject is not at rest, as observed in the fear tests.

Nonetheless, the updated approach provided high correlation results, and it showed that the computed HRV is deviated from the ECG results. In summary, radar front-ends with low carriers are not indicated to be used in the HRV assessment, since the mechanical heart displacement does not provide enough resolution to accurately identify the cardiac peaks and their exact time location.

One should mention that the cardiac models developed in this work mitigated external disruptive sources that might occurred in these specific scenarios. Therefore, if the surrounding conditions change or if the subjects present a more unstable behavior, a new model must be determined. Furthermore, despite this evaluation was performed in a CW radar, we believe that the same procedure can be conducted for the signals acquired with different radars operating with other carriers, such as frequency-modulated CW (FMCW) or pulsed radars. The presented method can also be used for other purposes, for instance, to evaluate the interindividual variability for biometric applications.

References

[1] C. Gouveia, D. Albuquerque, J. Vieira, and P. Pinho, "Dynamic digital signal processing algorithm for vital signs extraction in continuous-wave radars," *Remote Sens.*, vol. 13, no. 20, p. 4079, Oct. 2021.

[2] O. Boric-Lubecke, V. Lubecke, A. Droitcour, B. Park, and A. Singh, *Doppler Radar Physiological Sensing*. Hoboken, NJ, USA: Wiley, 2015.

[3] J. Tu and J. Lin, "Respiration harmonics cancellation for accurate heart rate measurement in non-contact vital sign detection," in *IEEE MTT-S Int. Microw. Symp. Dig.*, Jun. 2013, pp. 1–3.

[4] V. Das, A. Boothby, R. Hwang, T. Nguyen, J. Lopez, and D. Y. C. Lie, "Antenna evaluation of a non-contact vital signs sensor for continuous heart and respiration rate monitoring," in *Proc. IEEE Top. Conf. Biomed. Wireless Technol., Netw., Sens. Syst. (BioWireleSS)*, Jan. 2012, pp. 13–16.

[5] I. Mostafanezhad, E. Yavari, O. Boric-Lubecke, V. M. Lubecke, and D. P. Mandic, "Cancellation of unwanted Doppler radar sensor motion using empirical mode decomposition," *IEEE Sensors J.*, vol. 13, no. 5, pp. 1897–1904, May 2013.

[6] F. Weishaupt, I. Walterscheid, O. Biallawons, and J. Klare, "Vital sign localization and measurement using an LFMCW MIMO radar," in *Proc. 19th Int. Radar Symp. (IRS)*, Bonn, Germany, Jun. 2018, pp. 1–8.

[7] W. Hu, Z. Zhao, Y. Wang, H. Zhang, and F. Lin, "Noncontact accurate measurement of cardiopulmonary activity using a compact quadrature Doppler radar sensor," *IEEE Trans. Biomed. Eng.*, vol. 61, no. 3, pp. 725–735, Mar. 2014.

[8] S. Tomii and T. Ohtsuki, "Heartbeat detection by using Doppler radar with wavelet transform based on scale factor learning," in *Proc. IEEE Int. Conf. Commun. (ICC)*, Jun. 2015, pp. 483–488.

[9] X. Li, B. Liu, Y. Liu, J. Li, J. Lai, and Z. Zheng, "A novel signal separation and de-noising technique for Doppler radar vital signal detection," *Sensors*, vol. 19, no. 21, p. 4751, Nov. 2019.

[10] Y. I. Jang, J. Y. Sim, J.-R. Yang, and N. K. Kwon, "The optimal selection of mother wavelet function and decomposition level for denoising of DCG signal," *Sensors*, vol. 21, no. 5, p. 1851, Mar. 2021.

[11] M. Li and J. Lin, "Wavelet-transform-based data-length-variation technique for fast heart rate detection using 5.8-GHz CW Doppler radar," *IEEE Trans. Microw. Theory Techn.*, vol. 66, no. 1, pp. 568–576, Jan. 2018.

[12] T. K. V. Dai *et al.*, "Enhancement of remote vital sign monitoring detection accuracy using multiple-input multiple-output 77 GHz FMCW radar," *IEEE J. Electromagn., RF Microw. Med. Biol.*, vol. 6, no. 1, pp. 111–122, Mar. 2022.

[13] C. Gouveia, D. Albuquerque, P. Pinho, and J. Vieira, "Evaluation of heartbeat signal extraction methods using a 5.8 GHz Doppler radar system in a real application scenario," *IEEE Sensors J.*, vol. 22, no. 8, pp. 7979–7989, Apr. 2022.

[14] A. Aubert *et al.*, "Laser method for recording displacement of the heart and chest wall," *Med. Eng. Phys.*, vol. 6, no. 2, pp. 134–140, 1984.

[15] G. Ramachandran and M. Singh, "Three-dimensional reconstruction of cardiac displacement patterns on the chest wall during the P, QRS and T-segments of the ECG by laser speckle inteferometry," *Med. Biol. Eng. Comput.*, vol. 27, no. 5, pp. 525–530, Sep. 1989.

[16] C. Li, Y. Xiao, and J. Lin, "Design guidelines for radio frequency non-contact vital sign detection," in *Proc. 29th Annu. Int. Conf. IEEE Eng. Med. Biol. Soc.*, Aug. 2007, pp. 1651–1654.

[17] M. Kaisti *et al.*, "Stand-alone heartbeat detection in multidimensional mechanocardiograms," *IEEE Sensors J.*, vol. 19, no. 1, pp. 234–242, Jan. 2019.

[18] A. LoMauro and A. Aliverti, "Sex differences in respiratory function," *Breathe*, vol. 14, no. 2, pp. 131–140, Jun. 2018.

[19] S. Laborde, E. Mosley, and J. F. Thayer, "Heart rate variability and cardiac vagal tone in psychophysiological research—Recommendations for experiment planning, data analysis, and data reporting," *Frontiers Psychol.*, vol. 8, p. 213, Feb. 2017.

[20] F. Shaffer and J. P. Ginsberg, "An overview of heart rate variability metrics and norms," *Frontiers Public Health*, vol. 5, p. 258, Sep. 2017.

[21] J.-Y. Kim, J.-H. Park, S.-Y. Jang, and J.-R. Yang, "Peak detection algorithm for vital sign detection using Doppler radar sensors," *Sensors*, vol. 19, no. 7, p. 1575, Apr. 2019.

[22] W. Massagram, V. M. Lubecke, A. Høst-Madsen, and O. Boric-Lubecke, "Assessment of heart rate variability and respiratory sinus arrhythmia via Doppler radar," *IEEE Trans. Microw. Theory Techn.*, vol. 57, no. 10, pp. 2542–2549, Oct. 2009.

[23] N. T. Phuong Nguyen, P.-Y. Lyu, M. H. Lin, C.-C. Chang, and S.-F. Chang, "A short-time autocorrelation method for noncontact detection of heart rate variability using CW Doppler radar," in *IEEE MTT-S Int. Microw. Symp. Dig.*, May 2019, pp. 1–4.

[24] V. L. Petrović, M. M. Janković, A. V. Lupšić, V. R. Mihajlović, and J. S. Popović-Bovović, "High-accuracy real-time monitoring of heart rate variability using 24 GHz continuous-wave Doppler radar," *IEEE Access*, vol. 7, pp. 74721–74733, 2019.

[25] E. Turppa, J. M. Kortelainen, O. Antropov, and T. Kiuru, "Vital sign monitoring using FMCW radar in various sleeping scenarios," *Sensors*, vol. 20, no. 22, p. 6505, Nov. 2020.

[26] S. Suzuki, T. Matsui, S. Gotoh, Y. Mori, B. Takase, and M. Ishihara, "Development of non-contact monitoring system of heart rate variability (HRV)—An approach of remote sensing for ubiquitous technology," in *Ergonomics and Health Aspects of Work With Computers*. New York, NY, USA: Springer, 2009, pp. 195–203.

[27] W. Xia, Y. Li, and S. Dong, "Radar-based high-accuracy cardiac activity sensing," *IEEE Trans. Instrum. Meas.*, vol. 70, pp. 1–13, 2021.

[28] S. Vaseghi, "Wiener filters," in *Advanced Digital Signal Processing and Noise Reduction*. Cham, Switzerland: Springer-Verlag, 1996.

[29] J.-G. Kim, S.-H. Sim, S. Cheon, and S. Hong, "24 GHz circularly polarized Doppler radar with a single antenna," in *Proc. Eur. Microw. Conf.*, 2005, vol. 2, no. 4, p. 4.

[30] T. M. Shen, T. Y. J. Kao, T. Y. Huang, J. Tu, J. Lin, and R. B. Wu, "Antenna design of 60-GHz micro-radar system-in-package for noncontact vital sign detection," *IEEE Antennas Wireless Propag. Lett.*, vol. 11, pp. 1702–1705, 2012.

[31] C. Gouveia, A. Tomé, F. Barros, S. C. Soares, J. Vieira, and P. Pinho, "Study on the usage feasibility of continuous-wave radar for emotion recognition," *Biomed. Signal Process. Control*, vol. 58, Apr. 2020, Art. no. 101835.

[32] D. Batista, H. P. D. Silva, A. Fred, C. Moreira, M. Reis, and H. A. Ferreira, "Benchmarking of the BITalino biomedical toolkit against an established gold standard," *Healthcare Technol. Lett.*, vol. 6, no. 2, pp. 32–36, Apr. 2019.

[33] P. Kathirvel, M. S. Manikandan, S. R. M. Prasanna, and K. P. Soman, "An efficient R-peak detection based on new nonlinear transformation and first-order Gaussian differentiator," *Cardiovascular Eng. Technol.*, vol. 2, no. 4, pp. 408–425, 2011.

[34] B. Park, O. Boric-Lubecke, and V. M. Lubecke, "Arctangent demodulation with DC offset compensation in quadrature Doppler radar receiver systems," *IEEE Trans. Microw. Theory Techn.*, vol. 55, no. 5, pp. 1073–1079, May 2007.

[35] F. Shaffer, R. McCraty, and C. L. Zerr, "A healthy heart is not a metronome: An integrative review of the heart's anatomy and heart rate variability," *Frontiers Psychol.*, vol. 5, p. 1040, Sep. 2014.

Carolina Gouveia (Graduate Student Member, IEEE) received the first Licenciatura degree in health equipment technologies from the Polytechnical Institute of Leiria, Leiria, Portugal, in 2011, and master's degree in electronics and telecommunication engineering from the University of Aveiro, Aveiro, Portugal, in 2017, where she is currently pursuing the Ph.D. degree in electrical engineering, focusing on non-contact vital signs acquisition using radar systems.

She is currently a Researcher with the Radio Systems Group, Instituto de Telecomunicações (IT), Aveiro. Her research work led to six journal articles and three international conferences.

Ms. Gouveia received the Prize ANACOM-URSI Portugal in 2021, the EuMA 1st Prize at the Young Scientist Contest in MIKON Conference 2020, and the 2nd Award Fraunhofer Portugal Challenge in 2018. She was involved in the research project TexBoost: less Commodities more Specialities, which aimed to develop a smart seat cover, integrating a bio-radar system. This project led to a patent submission.

Daniel Filipe Albuquerque received the Diploma degree in electronics and telecommunications engineering and the Ph.D. degree in electrical engineering from the University of Aveiro, Aveiro, Portugal, in 2007 and 2013, respectively.

He was an Assistant Lecturer (2011–2013), a Visiting Professor (2013–2019), and an Assistant Professor (since 2019) with the School of Technology and Management of Viseu (Polytechnic Institute of Viseu), Viseu, Portugal, where he is also a member of the Research Centre in Digital Services (CISeD). His main research interest is in the development of signal processing tools to location and radar systems.

Dr. Albuquerque received the Prize ANACOM-URSI Portugal in 2021, the 1st Plug Prize from APRITEL in 2010, and the 3rd Prize in Technological Realization in Audio Engineering from the Portuguese section of Audio Engineering Society in 2007.

Pedro Pinho (Senior Member, IEEE) was born in Vale de Cambra, Portugal, in 1974. He received the Licenciado and master's degrees in electrical and telecommunications engineering and the Ph.D. degree in electrical engineering from the University of Aveiro, Aveiro, Portugal, in 1997, 2000, and 2004, respectively.

He is currently an Assistant Professor with the Department of Electronics, Telecommunications and Informatics Engineering, University of Aveiro (UA), and a Senior Member of the research staff in the Instituto de Telecomunicaç oes (IT), Aveiro. He has authored or coauthored one book, ten book chapters, and more than 100 papers for conferences and international journals. He participated as a principal investigator or a coordinator in projects with scientific and/or industry focus, both at a national and international level. To date, he has led and leads eight Ph.D. students and 60 M.Sc. students. His current research interests are in optical systems and antennas.

Dr. Pinho serves as a Technical Program Committee member of several conferences, a reviewer for several IEEE journals, and a member of the IEEE APS.

José Vieira received the B.Sc. degree in electrical engineering and the M.Sc. degree in systems and automation from the University of Coimbra, Coimbra, Portugal, in 1988 and 1993, respectively, and the Ph.D. degree in electrical engineering from the University of Aveiro, Aveiro, Portugal, in 2000.

Since then, he has been an Assistant Professor with the University of Aveiro. His main research interests are digital audio signal processing, ultrasonic location, software-defined radio, all-digital radio front-ends, and radar.

Dr. Vieira founded the AES Portuguese Section in 2004 and its President from 2005 to 2011. In 2010, we won the Plug Award from APRITEL with the "Bio-inspired cochlear radio."